Angewandte Chemie
Eine Zeitschrift der Gesellschaft Deutscher Chemiker

Supporting Information

69451 Weinheim, Germany

Transient X-ray Diffraction Reveals Global and Major Reaction Pathways for Iodoform in Solution

Jae Hyuk Lee[1], Joonghan Kim[1], Marco Cammarata[2], Qingyu Kong[2], Kyung Hwan Kim[1], Jungkweon Choi[1], Tae Kyu Kim[3], Michael Wulff[2], and Hyotcherl Ihee[1]*

[1]*National Creative Research Initiative Center for Time-Resolved Diffraction, Department of Chemistry and School of Molecular Science (BK21), Korea Advanced Institute of Science and Technology (KAIST), Daejeon, 305-701, Republic of Korea*

[2]*European Synchrotron Radiation Facility (ESRF), BP220, Grenoble Cedex 38043, France*

[3]*Department of Chemistry and Chemistry Institute for Functional Materials, Pusan National University, Pusan, 609-735, (Republic of Korea)*

Three components for all time delays and peak assignment

Based on the global fitting results for change in populations and the solvent's temperature and density, we can plot the difference diffraction intensity, $q\Delta S(q,t)$, for the three principal components (solute-only term, solute/solvent cross term, and solvent-only term) for all time delay in reciprocal space (Fig. S1). The radial Fourier transform of the curves in Fig. S1 gives the difference radial distribution, $r\Delta S(r,t)$, for the three components (Fig. S2). Peaks are assigned in the bottom part of Fig. S2. It clearly shows that the peak around 6 Å in Fig. 1b is from the solvent density change, not isomer formation, and the peak around 2 Å is also from the solvent density change, not related with the formation of I_2.

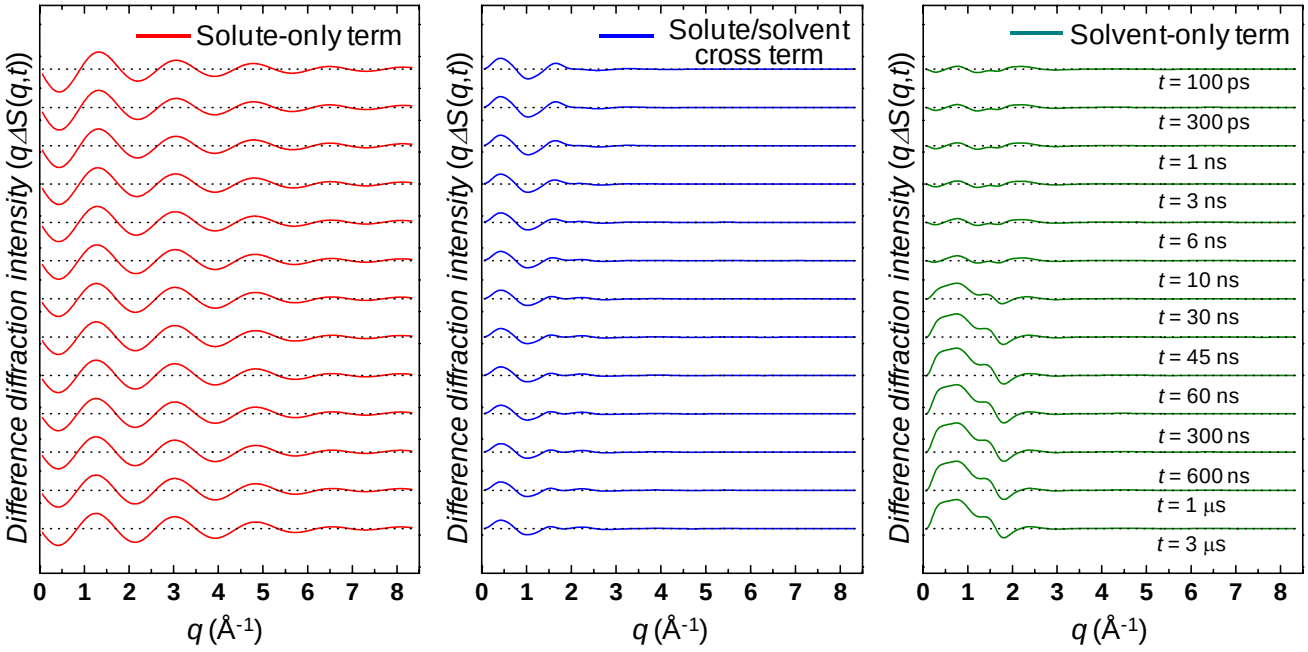

Figure S1. Decomposition to the three principal components (solute-only term, solute/solvent cross term, and solvent-only term) of difference diffraction signal, $q\Delta S(q,t)$, as a function of time-delay for iodoform in methanol solution. Left: Difference diffraction intensities, $q\Delta S(q,t)$, for the solute-only term at each time-delay (red). Center: $q\Delta S(q,t)$ for the solute/solvent cross term (blue). Right: $q\Delta S(q,t)$ for the solvent-only term (green).

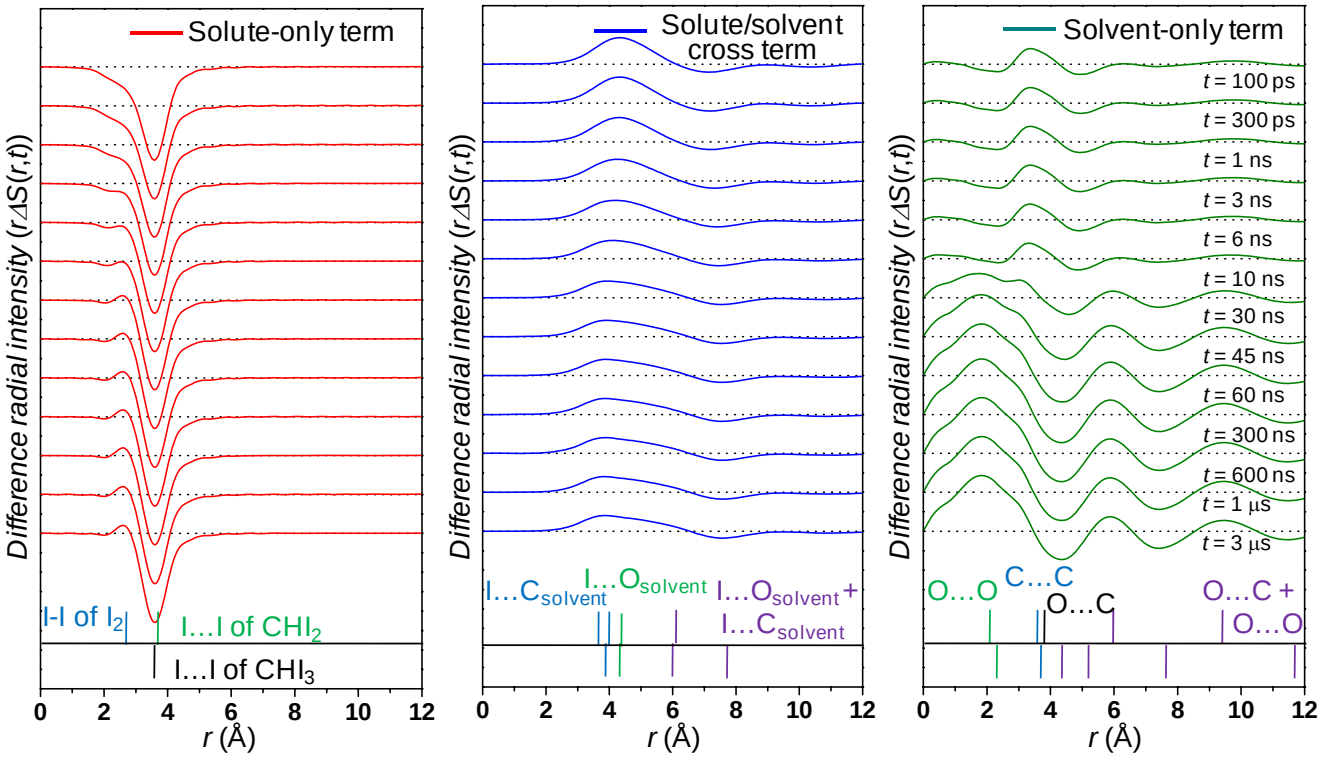

Figure S2. Real-space decomposition to the three components (solute-only term, solute/solvent cross term, and solvent-only term) in the difference radial intensity, *rΔS(r,t)*, as a function of time-delay for iodoform in liquid methanol. Left: Difference radial intensities, *rΔS(r,t)*, for the solute-only term at each time-delay (red). Center: *rΔS(r,t)* for the solute/solvent cross term (blue). Right: *rΔS(r,t)* for the solvent-only term (green). The peak assignments for atom-atom pairs are also shown in the bottom of each panel. The peak around 6 Å in Fig. 1b is from the solvent density change, not isomer formation, and the peak around 2 Å is also from the solvent density change, not related with I_2 formation.

Global fit results with isomers of various C-I-I angles

In addition to the optimized isomer structure with C-I-I angle of 134°, isomer structures with various C-I-I angles ranging from 134° to 90° were tested in the global fitting analysis. The energy scan from 134° to 90° by using DFT calculation shown in Fig. S3 clearly indicate that the isomer structure with C-I-I angles less than 134° becomes energetically less favorable. For the global fitting analysis, isomer structures with four additional C-I-I angles (90°, 105°, 115°, and 125°) were used. The distances between iodine atoms in each molecule are 3.68 Å, 3.59 Å, and 4.88 Å for 90°, 3.41 Å, 3.59 Å, and 5.36 Å for 105°, 3.32 Å, 3.60 Å, and 5.68 Å for 115°, and 3.31 Å, 3.61 Å, and 5.94 Å for 125°. In

the free floating condition of each parameter, the fraction of isomers converged to zero. For the sake of comparison, we fixed the parameter related with the existence of isomer according to previous literatures. The χ^2 values at 10 ns show anti-correlation to the C-I-I angles, and all χ^2 values from isomers are greater than that from the radical channel (Fig S4).

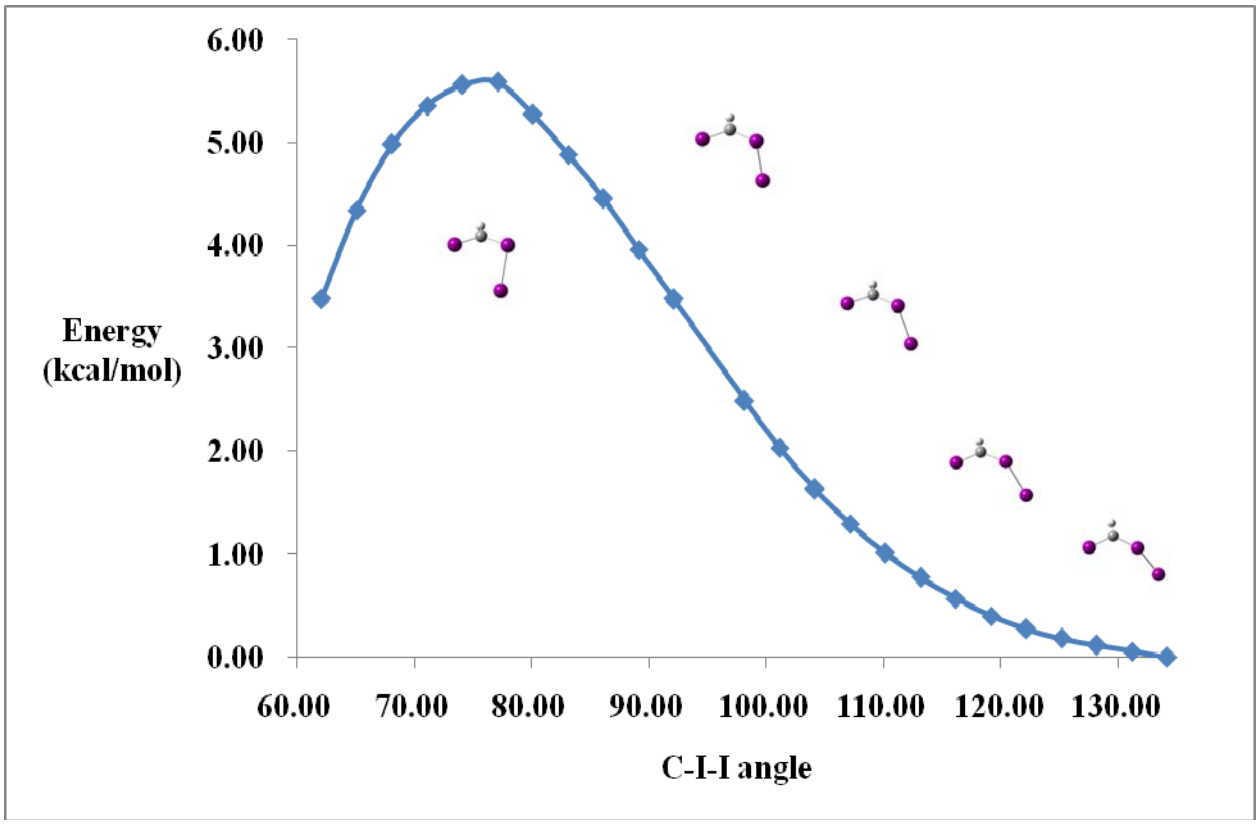

Figure S3. Energy profile of CH_2I-I structure as a function of the C-I-I angle. Energies were calculated using B3LYP/6-311++G(d,p) with IEFPCM method. All structural parameters were optimized except C-I-I angle.

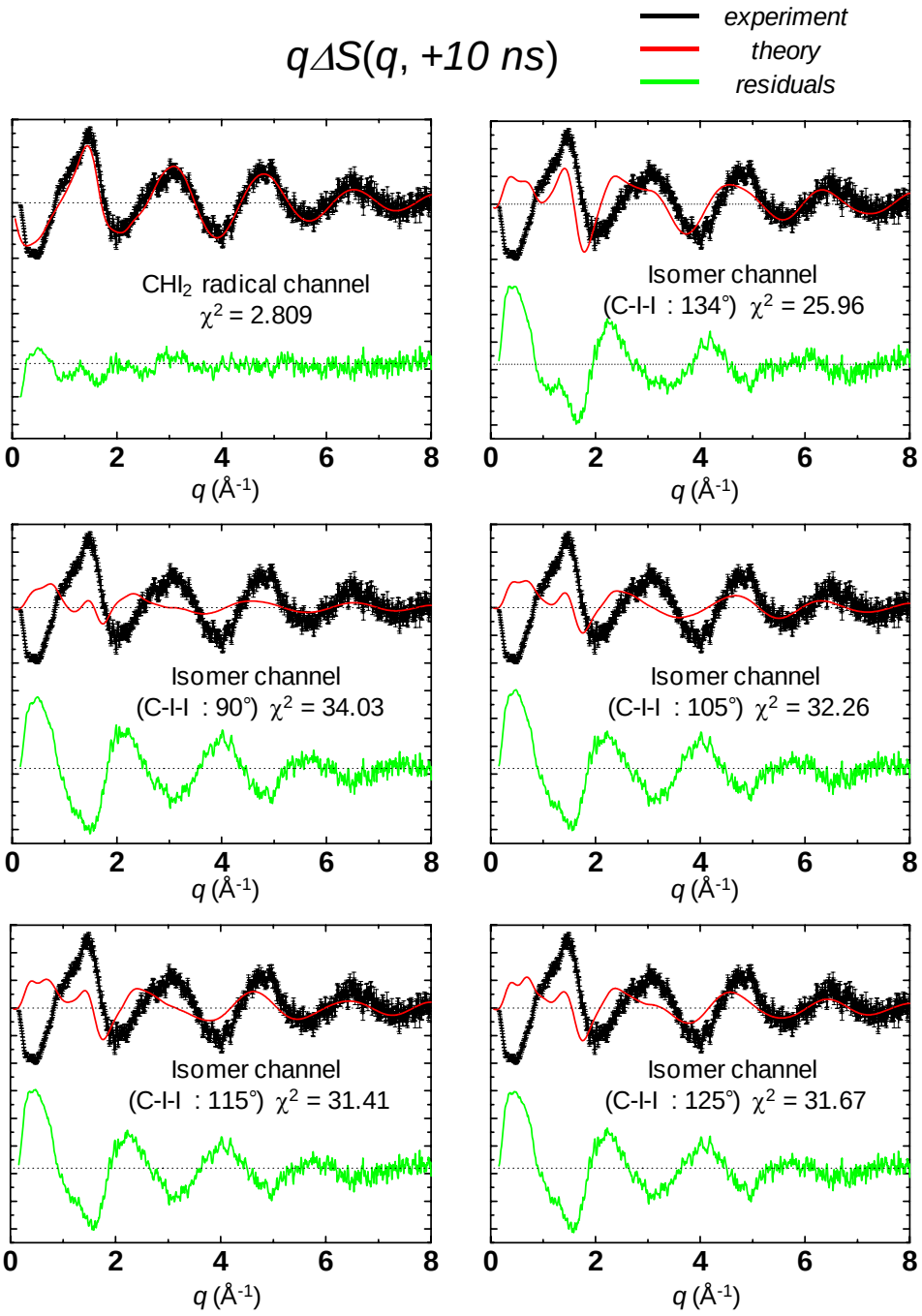

Figure S4. Global fit analysis results at 10 ns time delay. Fit results from Hypothetical isomers are worse than the result from the radical channel and the stable isomer channel.

Supporting table

Table S1. The XYZ coordinates (Å) and absolute energy (hartree) of CHI_3 calculated using B3LYP/6-311++G(d,p) level.

CHI_3 (C_{3V})	X	Y	Z
C	0.000000	0.000000	0.551462
H	0.000000	0.000000	1.634213
I	0.000000	2.088328	-0.031088
I	1.808545	-1.044164	-0.031088
I	-1.808545	-1.044164	-0.031088
Energy		-20797.29649220	
E + ZPE		-20797.279844	

Table S2. The XYZ coordinates (Å) and absolute energy (hartree) of CHI_2-I calculated using B3LYP/6-311++G(d,p) level.

CHI_2-I (C_1)	X	Y	Z
C	1.604715	0.653808	0.703498
H	1.750716	0.970611	1.737347
I	-0.189943	1.004093	-0.093563
I	3.077709	-0.543953	-0.042308
I	-3.102464	-0.552469	0.023449
Energy		-20797.26050360	
E + ZPE		-20797.245673	

Table S3. The XYZ coordinates (Å) and absolute energy (hartree) of CHI_2 calculated using B3LYP/6-311++G(d,p) level.

CHI_2 (C_S)	X	Y	Z
C	-0.002603	0.901726	0.000000
H	0.291502	1.946322	0.000000
I	-0.002603	-0.069403	1.828335
I	-0.002603	-0.069403	-1.828335
Energy		-13877.72250080	
E + ZPE		-13877.709344	

Table S4. The XYZ coordinates (Å) and absolute energy (hartree) of CHI calculated using B3LYP/6-311++G(d,p) level.

CHI (C_S)	X	Y	Z
C	0.018169	1.822814	0.000000
H	-1.071954	2.040725	0.000000
I	0.018169	-0.244861	0.000000
Energy		-6958.11650379	
E + ZPE		-6958.106142	

References

T. K. Kim, M. Lorenc, J. H. Lee, M. Russo, J. Kim, M. Cammarata, Q. Y. Kong, S. Noel, A. Plech, M. Wulff, H. Ihee, *Proc. Nat.l Acad. Sci. USA.* **2006**, *103*, 9410.

J. Davidsson, J. Poulsen, M. Cammarata, P. Georgiou, R. Wouts, G. Katona, F. Jacobson, A. Plech, M. Wulff, G. Nyman, R. Neutze, *Phys. Rev. Lett.* **2005**, *94*.

M. Cammarata, M. Lorenc, T. K. Kim, J. H. Lee, Q. Y. Kong, E. Pontecorvo, M. Lo Russo, G. Schiro, A. Cupane, M. Wulff, H. Ihee, *J. Chem. Phys.* **2006**, *124*.

Gaussian03 (Revision A.1) M. J. Frisch, H. B. Schlegel, G. E. Scuseria, M. A. Robb, J. R. Cheeseman, J. A. Montgomery, Jr., T. Vreven, K. N. Kudin, J. C. Burant, J. M. Millam, S. S. Iyengar, J. Tomasi, V. Barone, B. Mennucci, M. Cossi, G. Scalmani, N. Rega, G. A. Petersson, H. Nakatsuji,

M. Hada, M. Ehara, K. Toyota, R. Fukuda, J. Hasegawa, M. Ishida, T. Nakajima, Y. Honda, O. Kitao, H. Nakai, M. Klene, X. Li, J. E. Knox, H. P. Hratchian, J. B. Cross, V. Bakken, C. Adamo, J. Jaramillo, R. Gomperts, R. E. Stratmann, O. Yazyev, A. J. Austin, R. Cammi, C. Pomelli, J. W. Ochterski, P. Y. Ayala, K. Morokuma, G. A. Voth, P. Salvador, J. J. Dannenberg, V. G. Zakrzewski, S. Dapprich, A. D. Daniels, M. C. Strain, O. Farkas, D. K. Malick, A. D. Rabuck, K. Raghavachari, J. B. Foresman, J. V. Ortiz, Q. Cui, A. G. Baboul, S. Clifford, J. Cioslowski, B. B. Stefanov, G. Liu, A. Liashenko, P. Piskorz, I. Komaromi, R. L. Martin, D. J. Fox, T. Keith, M. A. Al-Laham, C. Y. Peng, A. Nanayakkara, M. Challacombe, P. M. W. Gill, B. Johnson, W. Chen, M. W. Wong, C. Gonzalez, and J. A. Pople, in *Gaussian, Inc*, Wallingford CT, **2004**.